

# Selective determination of free dissolved chlorine using nitrogen-doped carbon dots as a fluorescent probe

Yanping Lin<sup>1,2</sup> · Bixia Yao<sup>1,2</sup> · Tingting Huang<sup>1,2</sup> · Shichao Zhang<sup>1,2</sup> · Xiaotong Cao<sup>1,2</sup> · Wen Weng<sup>1,2</sup>

Received: 16 January 2016 / Accepted: 23 April 2016 / Published online: 4 May 2016  
© Springer-Verlag Wien 2016

**Abstract** The authors report that nitrogen-doped carbon dots (N-CDs) represent a viable fluorescent probe for the determination of dissolved free chlorine. The N-CDs can be fairly easily prepared by a solvothermal method using citric acid, tartaric acid and ethanediamine as the precursors, display excitation/emission maxima of 360/460 nm, and have a quantum yield of 42.2 %. Free chlorine and  $\text{ClO}^-$  quench fluorescence, and this was exploited to design a method for fluorometric determination of chlorine and hypochlorite. The probe has a short response time ( $< 1$  min), excellent selectivity, high sensitivity, and a linear response range that extends from 0.1 to 27  $\mu\text{M}$ . The limit of detection is as low as 29.7 nM. The method was applied to the determination of chlorine dissolved in tap water.

**Keywords** Nanoparticles · Nanomaterial · Carbonization · Fluorescence quenching · Fluorescence decay · Quantum yield · High resolution transmission electron microscopy · XPS · Hypochlorite · Water analysis

## Introduction

Chlorine ( $\text{Cl}_2$ ), hypochlorous acid ( $\text{HClO}$ ), and hypochlorite ( $\text{ClO}^-$ ) are extensively used as disinfectants due to their strong oxidizing property. The sum of dissolved

$\text{Cl}_2$ ,  $\text{HClO}$ , and  $\text{ClO}^-$  in water is defined as free residual chlorine [1]. The concentration of free chlorine should be neither too low nor too high. Too low-level free chlorine cannot kill pathogenic bacteria and viruses in water effectively. However, too high-level free chlorine would react with organic materials existing in water to produce chlorinated byproducts, which have been reported to be potentially harmful to human beings and animals [2]. Concentrated free chlorine solutions can cause respiratory problems, skin and throat irritation, abdominal pain, burning sensations, coughing, and vomiting [3]. Therefore, it is typically controlled at concentrations between  $10^{-5}$  and  $10^{-2}$   $\text{mol}\cdot\text{L}^{-1}$  in our daily life [4]. It is necessary to monitor and control the level of chlorine in water.

Many methods have been reported for the determination of free chlorine, including the well known iodometric titration [5], colorimetry [6], chemiluminescence [7–9], ion chromatography [10], gas chromatography [2], liquid chromatography [11], flow injection analysis [12], and so on. Though each method has its advantages, many reported means still involve low detection sensitivity, poor selectivity, the use of toxic reagents, or the employ of complicated performance. Developing facile and effective methods for the determination of free chlorine is still of significance.

The applications of carbon dots in the field of bioimaging, biosensing, ions detection, optoelectronic devices and photocatalysis have attracted much attention. A fluorescent probe based on nitrogen-doped carbon dots was prepared and applied in the determination of free chlorine in this report. The obtained N-CDs exhibited excellent selectivity and sensitivity of fluorescence quenching for free chlorine, and possessed promising potential applications in the detection of free chlorine in real water samples.

✉ Wen Weng  
weng\_wen@126.com

<sup>1</sup> College of Chemistry and Environment, Minnan Normal University, Zhangzhou 363000, China

<sup>2</sup> Fujian Provincial Key Laboratory of Modern Analytical Science and Separation Technology, Zhangzhou 363000, China

## Experimental

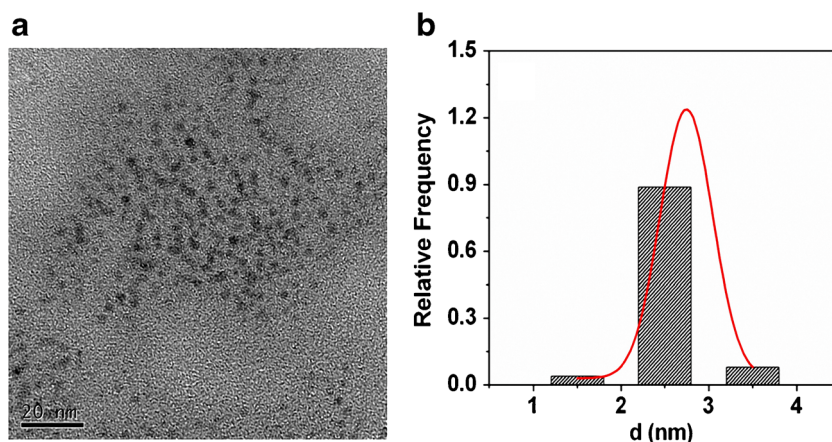
### Chemicals

Citric acid monohydrate (CA), *L*-tartaric acid, ethanediamine and oleic acid were all analytical reagents (AR). They were purchased from Shanghai Sinopharm Chemical Reagent Co. Ltd. (Shanghai, China; [www.reagent.com.cn](http://www.reagent.com.cn)). Quinine sulfate was purchased from Aladdin Industrial Corporation (Shanghai, China; [www.aladdin-e.com](http://www.aladdin-e.com)). Ultrapure water was prepared with a Milli-Q system (Millipore, Bedford, MA, USA; [www.merckmillipore.com](http://www.merckmillipore.com)). Sodium hypochlorite solution with a concentration of 1.37 M was purchased from Xilong Chemical Co. Ltd. (Guangdong, China; [www.xlhg.com](http://www.xlhg.com)). Other reagents were all analytical and were used without further purification.

### Apparatus

A UV-2550 spectrophotometer (Shimadzu; [www.shimadzu.com](http://www.shimadzu.com)) was used to record UV–vis spectra of the N-CDs. The fluorescence spectra were obtained by a Varian Cary Eclipse Fluorescence Spectrophotometer (Varian; [www.agilent.com.cn](http://www.agilent.com.cn)). Fluorescence decay was measured by an Edingburgh Instruments FLS920 fluorescence spectrometer (Edingburgh Instruments; [www.edinst.com](http://www.edinst.com)). Transmission electron microscopy (TEM) and high-resolution TEM (HRTEM) images were recorded using FEI Tecnai G2 F20 instruments (FEI; [www.fei.com](http://www.fei.com)). The X-ray photoelectron spectroscopy (XPS) spectra were recorded using a Thermo ESCALAB 250Xi multifunctional imaging electron spectrometer (Thermo Fisher; [www.thermoscientific.com](http://www.thermoscientific.com)). Elemental analysis was performed using a vario EL Elemental Analyzer (Elementar Analysensysteme GmbH, Germany; [www.elementar.de](http://www.elementar.de)).

**Fig. 1** The TEM image (a) and the size distribution (b) of the N-CDs



### Preparation of the N-CDs

A simple one-step solvothermal method was used to prepare the mentioned N-CDs. A typical synthesis process is as follows. CA monohydrate (1.5 g) and *L*-tartaric acid (1.5 g) were placed in a three neck flask, and then ethanediamine (5 mL) and oleic acid (30 mL) were added. The mixture was then heated at 220 °C for 30 min under vigorous magnetic stirring. The colorless solution changed to a clear brownish black solution as the reaction progressed. After the reaction, the solution was cooled at room temperature, and then black solid precipitate was obtained directly. The precipitate was washed sufficiently with *n*-hexane, dispersed in ultrapure water, and centrifuged at 6000 rpm (centrifugation force, 5000 g) for 30 min to remove large particles product.

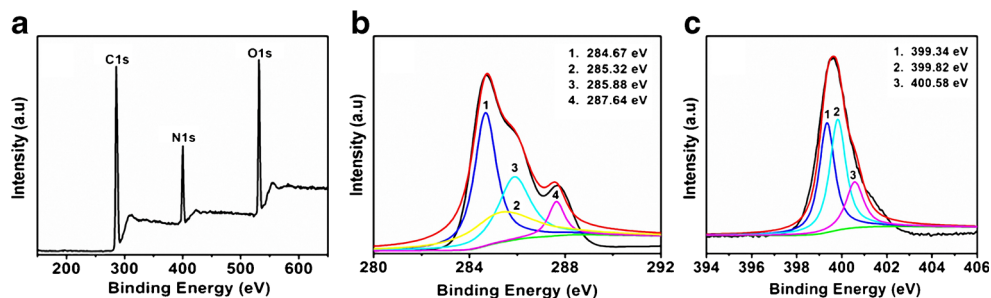
### Calculation of quantum yield of the N-CDs

The quantum yield (QY) of the obtained N-CDs was measured by comparing the integrated photoluminescence (PL) intensities and the absorbance value of the product with the reference quinine sulfate. The quinine sulfate (literature  $QY_R = 0.54$  at an excitation wavelength of 360 nm) was dissolved in 0.1 M  $H_2SO_4$  (refractive index  $\eta$  of 1.33), and the obtained N-CDs were dissolved in ultrapure water ( $\eta = 1.33$ ). Absorbencies in the 10 mm fluorescence cuvette were kept under 0.1 at the excitation wavelengths. The quantum yield of the N-CDs was determined by the following equation:

$$QY = QY_R \times \frac{I}{I_R} \times \frac{A_R}{A} \times \frac{\eta^2}{\eta_R^2}$$

where  $I$  is the measured integrated emission intensity,  $\eta$  is the refractive index of the solvents, and  $A$  is the optical density. The subscript  $R$  refers to the reference of known quantum yield.

**Fig. 2** The XPS spectrum of the obtained N-CDs (**a**). **b** and **c** are the corresponding  $C_{1s}$  spectrum and  $N_{1s}$  spectrum



## Results and discussion

### Synthesis and characterization of the N-CDs

The N-CDs were prepared according to our previously reported method [13]. CA monohydrate, tartaric acid and ethanediamine were used as the precursors. Unlike hydrothermal method, oleic acid was used as the reaction media. The fabrication process did not use any inorganic acid or metal ion. Water generated in the reaction process may act as a “soft-template”, and modulate the size of the formed nanoparticles [14]. The TEM image (Fig. 1a) shows that the product was uniform sphere particles. The size distribution histogram (Fig. 1b) shows that the N-CDs had a narrow size distribution in the range of 1 to 4 nm, with an average diameter of about 2.66 nm. The high-resolution TEM (HRTEM) images of the N-CDs did not show any discernible lattice fringes, indicating the amorphous nature of the obtained N-CDs.

The product was characterized by X-ray photoelectron spectroscopy (XPS). The XPS spectrum shows three peaks at 286.05, 399.87 and 532.34 eV (Fig. 2a), which can be attributed to  $C_{1s}$ ,  $N_{1s}$ , and  $O_{1s}$ , respectively. The  $C_{1s}$  spectrum can be deconvoluted into four peaks at 284.67, 285.32, 285.88 and 287.64 eV (Fig. 2b), indicating the presence of four types of carbon bonds:  $sp^2 C = C$  or  $sp^3 C-C$ ,  $C-N$  or  $C-O$ ,  $sp^2 N-C = N$ , and  $C = O$ . The deconvolution of the  $N_{1s}$  spectrum indicated the presence of three types of nitrogen bonds:  $C-N-C$  (399.34 eV),  $N-(C)_3$  (399.82 eV), and  $C-N-H$  groups (400.58 eV) (Fig. 2c) [15]. The elemental analysis showed

that the product contained 38.97 % of carbon, 15.59 % of nitrogen, 6.70 % of hydrogen, and 38.74 % of oxygen (calculated) by weight. This suggests that the N-CDs contain rich nitrogen and oxygen. The oxygen- and nitrogen-containing functional groups such as hydroxyl group and amino group endow the product with good water-solubility.

The UV-vis spectrum (Fig. 3a) shows that there are two absorbance bands centered at 239 and 351 nm. The peak at 239 nm can be ascribed to the  $\pi-\pi^*$  transitions of the aromatic  $C = C sp^2$  domains which can not produce observed fluorescence signal [16, 17]. The other absorption peak at 351 nm can be ascribed to the trapping of excited state energy of the surface states, which can lead to strong fluorescence [18]. The fluorescent spectrum of the obtained N-CDs conformed to the UV-vis absorption features. Figure 3b shows that the emission peak remains essentially unchanged with the variation of excitation wavelength in the range of 320–400 nm. The excitation-independent emission associated with organic fluorophores was also reported by Giannelis et al. in a systematic investigation of the formation mechanism of carbogenic nanoparticles by the pyrolysis of citric acid and ethanolamine [19]. A redshift happened when the excitation wavelength was greater than 400 nm. The maximum emission peak was observed at 460 nm, at an excitation wavelength of 360 nm.

The product emitted bright blue color under 365 nm UV light (Fig. 3a, inset). The quantum yield (QY) of the obtained N-CDs was calculated to be 42.2 % using quinine sulfate as a reference. The reaction temperature was moderate and the operation process was easily controlled. The N-CDs can be

**Fig. 3** The UV-vis and photoluminescence spectrum (**a**) and the excitation-dependent emission spectrum (**b**) of the N-CDs. Inset of A, the photographs under illumination of white (left) and UV (365 nm, right) light

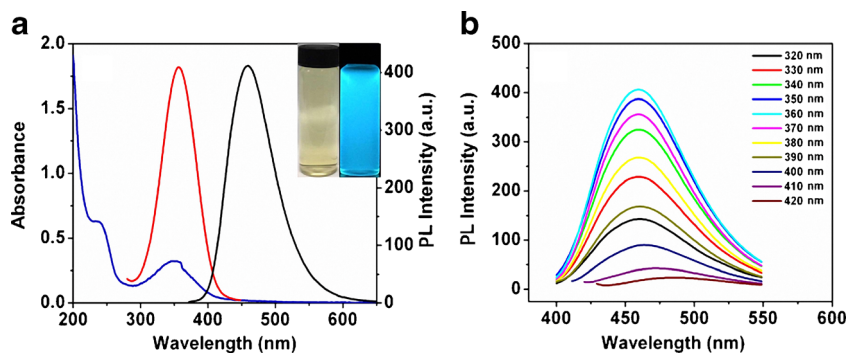
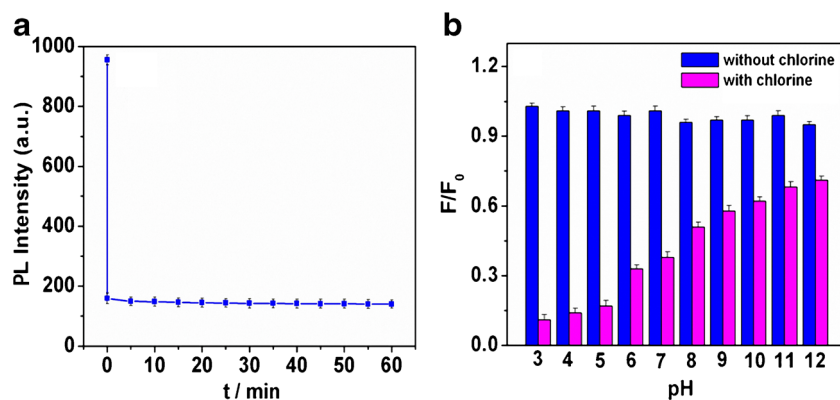


**Fig. 4** Time- (a) and pH-dependent (b) fluorescence response of the N-CDs with free chlorine. Concentration of the N-CDs,  $4.0 \mu\text{g}\cdot\text{mL}^{-1}$  for (a) and  $2.5 \mu\text{g}\cdot\text{mL}^{-1}$  for (b); concentration of sodium hypochlorite,  $25 \mu\text{M}$  for (a) and  $10 \mu\text{M}$  for (b)



obtained smoothly from batch to batch. The N-CDs exhibit low cytotoxicity, and have been applied to in vitro cell imaging [20]. We further explore their application in the determination of free chlorine.

### Fluorometric determination of free chlorine

To understand the response rate of the fluorescence signal of the N-CDs to free chlorine, the time-dependent fluorescence changes upon addition of  $25 \mu\text{M}$  hypochlorite were first monitored. As shown in Fig. 4a, the fluorescence intensity of the N-CDs at  $460 \text{ nm}$  was quenched by about 85 % as soon as the hypochlorite was added into the solution. The intensity kept basically stable during the following 60 min. This result suggests that the fluorescence quenching of free chlorine to the N-

CDs is quite rapid, implying their promising application in fast assay of free chlorine.

Another key factor for the determination is the pH value of solution. Figure 4b shows that the fluorescence intensity of the N-CDs in the absence of free chlorine remains basically unchanged with the variation of pH value. In contrast, the intensity had an obvious change in the presence of free chlorine with the variation of pH value. The intensity had a larger quenching in the lower pH value circumstance. The local pH value affects the chemical equilibrium between  $\text{HClO}$ ,  $\text{ClO}^-$  and chlorine. Free chlorine exists mainly as hypochlorous acid ( $\text{HClO}$ ) in acid, neutral and weakly alkaline solutions ( $\text{pH} = 3\text{--}9$ ), and as hypochlorite anion ( $\text{ClO}^-$ ) in strong alkaline solutions ( $\text{pH} > 9$ ) [21]. As  $\text{HClO}$  exhibits stronger oxidation capacity than  $\text{ClO}^-$  (redox potential is 1.63 V for the

**Fig. 5** a Normalized fluorescence of aqueous N-CDs solution ( $4.0 \mu\text{g}\cdot\text{mL}^{-1}$ ) in the presence of  $30 \mu\text{M}$  of various ions at  $360 \text{ nm}$  excitation wavelength. b Selective PL response of aqueous N-CDs solution towards  $20 \mu\text{M}$   $\text{ClO}^-$  (black bars), and interference of  $20 \mu\text{M}$  of other ions with  $20 \mu\text{M}$   $\text{ClO}^-$  (red bars). c The dependence of fluorescence intensity on the concentrations of  $\text{ClO}^-$  within the range of 0– $40 \mu\text{M}$ . d Fluorescence emission spectra of aqueous N-CDs solution upon addition of various concentrations of  $\text{ClO}^-$  (from top to bottom: 0, 0.1, 0.5, 1, 3, 6, 9, 12, 15, 18, 21, 24 and  $27 \mu\text{M}$ )

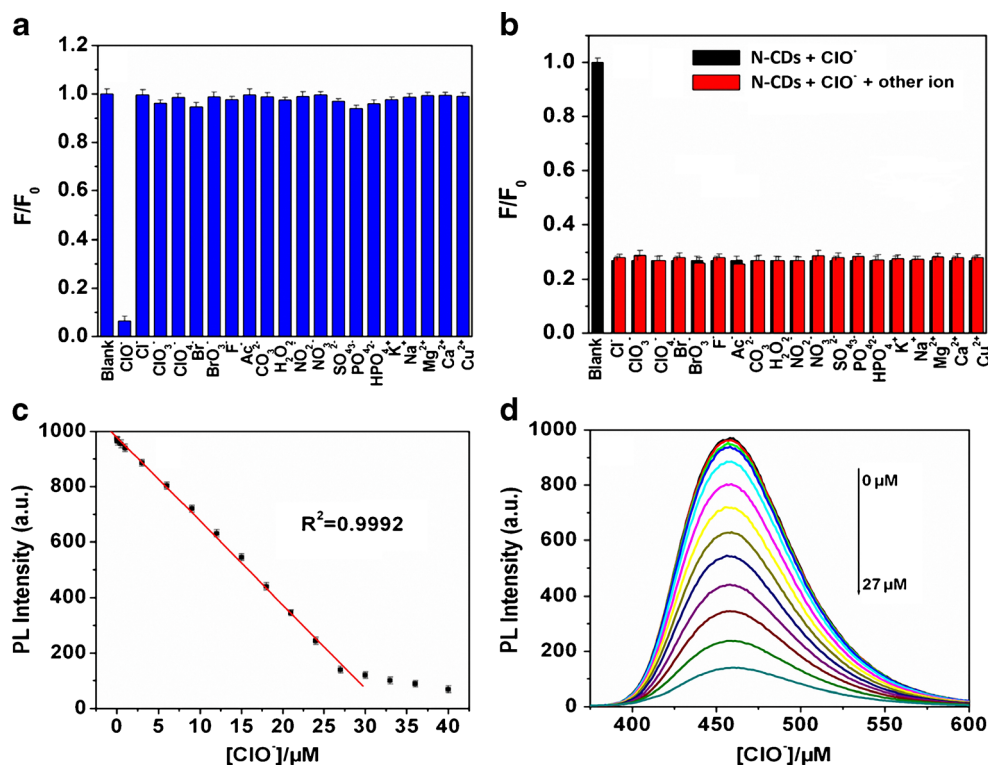




**Table 1** Figures of merit of recently reported methods for determination of free chlorine and hypochlorite

Material/method used	LOD ( $\mu\text{M}$ )	Linear range ( $\mu\text{M}$ )	Ref.
Graphene quantum dots/fluorescence	0.05	0.05–10	[1]
Carbon dots/fluorescence	0.015	0.2–2.0	[22]
Carbon dots/fluorescence	0.05	0.1–10	[23]
Carbon dot-rhodamine B nanohybrid/fluorescence	4	10–140	[24]
N,S-co-doped carbon dots/fluorescence	0.005	0.01–100	[25]
Graphene quantum dots/chemiluminescence	0.3	0.5–1000	[9]
Carbon nitride quantum dots/chemiluminescence	0.01	0.02–10	[26]
N-CDs/fluorescence	0.0297	0.1–27	This work

former, and 0.90 V for the latter), we think that oxidative process is the main reason for fluorescence quenching of the N-CDs with the addition of free chlorine. It is suitable to choose neutral environment for the convenience of experiments.

### Detection of free chlorine based on the N-CDs

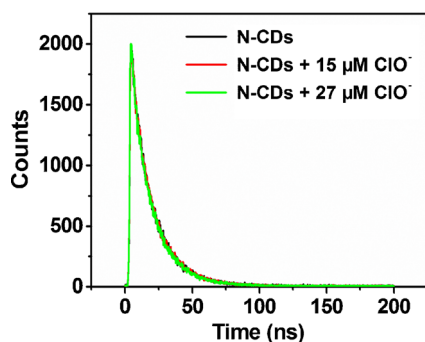
To evaluate the selectivity of the present assay system, two control experiments were performed. First, 30  $\mu\text{M}$  of various biologically and environmentally relevant ions, including  $\text{ClO}^-$ ,  $\text{Cl}^-$ ,  $\text{ClO}_3^-$ ,  $\text{ClO}_4^-$ ,  $\text{Br}^-$ ,  $\text{BrO}_3^-$ ,  $\text{F}^-$ ,  $\text{Ac}^-$ ,  $\text{CO}_3^{2-}$ ,  $\text{H}_2\text{O}_2$ ,  $\text{NO}_2^-$ ,  $\text{NO}_3^-$ ,  $\text{SO}_4^{2-}$ ,  $\text{PO}_4^{3-}$ ,  $\text{HPO}_4^{2-}$ ,  $\text{K}^+$ ,  $\text{Na}^+$ ,  $\text{Mg}^{2+}$ ,  $\text{Ca}^{2+}$  and  $\text{Cu}^{2+}$  were added into the N-CDs solution, and the PL responses were recorded. As shown in Fig. 5a, significant fluorescence quenching was observed with the addition of  $\text{ClO}^-$ , while the other ions showed only a negligible quenching effect. Lead ions ( $\text{Pb}^{2+}$ ) also had no discernible effect on the fluorescence, while mercury ions ( $\text{Hg}^{2+}$ ) had a medium impact.

In another control experiment, 20  $\mu\text{M}$  of  $\text{ClO}^-$  alone (black bars, Fig. 5b) and the mixtures of 20  $\mu\text{M}$  of  $\text{ClO}^-$  and 20  $\mu\text{M}$  of the above mentioned ions (red bars, Fig. 5b) were added into the aqueous N-CDs solution respectively, then the quenching effects were examined. From the results shown in Fig. 5b, we can see that the influence of other potentially

interfering ions on the fluorescence quenching is negligible. These observations indicate that the fluorescence quenching of the N-CDs is selective to  $\text{ClO}^-$  but insensitive to other common ions.

Concentration experiments show that the fluorescence intensity decreased gradually with the increase of the concentration of  $\text{ClO}^-$  ions. Figure 5c presents the intensity versus the concentration of  $\text{ClO}^-$ . There exists a good linear correlation ( $R^2 = 0.9992$ ) between the intensity and the concentration of  $\text{ClO}^-$  in the range of 0.1 to 27  $\mu\text{M}$ . The limit of detection (LOD) was estimated to be 29.7 nM based on three times the standard deviation rule ( $\text{LOD} = 3\text{Sd/s}$ ). Figure 5d shows the overlap fluorescence emission spectra of the N-CDs upon addition of various concentrations of  $\text{ClO}^-$ . It should be noted that the obtained limit of detection of the N-CDs for  $\text{ClO}^-$  detection is comparable or much lower than those previously reported with other fluorescent probes [1, 22–24]. Table 1 shows the figures of merit of recently reported methods for determination of free chlorine and hypochlorite. The results show that the present assay system exhibits superior selectivity and sensitivity to  $\text{ClO}^-$  ions, and may be useful in environmental applications for  $\text{ClO}^-$  detection.

In order to further explore the fluorescence quenching mechanism, effects of other commonly used oxidants on the fluorescence of the N-CDs were investigated. We found that

**Fig. 6** Fluorescence decay of aqueous N-CDs solutions at 360 nm excitation wavelength**Table 2** Determination of free chlorine and hypochlorite in tap water samples

	Found ( $\mu\text{M}$ )	Added ( $\mu\text{M}$ )	Total found ( $\mu\text{M}$ )	RSD (% , $n = 3$ )	Recovery (%)
Sample 1	0.71	0.50	1.23	3.34	104.0
		1.00	1.76	4.51	105.0
		3.00	3.58	4.12	95.7
		5.00	5.66	5.39	99.0
Sample 2	1.40	0.50	1.94	4.32	108.0
		1.00	2.37	4.78	97.0
		3.00	4.46	3.65	102.0
		5.00	6.19	5.11	95.8

the oxidants with stronger oxidation capability (such as  $\text{KMnO}_4$  and  $\cdot\text{OH}$ ) than free chlorine can also quench the fluorescence, while the other weaker oxidants (such as  $\text{H}_2\text{O}_2$ ,  $\text{Fe}^{3+}$ ) have nearly no or little effect on the fluorescence of the N-CDs. Though the exact mechanism of the fluorescence quenching of carbon dots by free chlorine is still not fully known, more and more evidence indicate that the fluorescence properties of carbon dots are affected significantly by their surface states [1, 27–29]. The surface of the obtained N-CDs contains large amounts of reductive hydroxyl groups due to incomplete carbonization. Free chlorine may destroy the surface passivation of the N-CDs, resulting in the quenching of the fluorescence.

In addition, fluorescence life times of the N-CDs were determined using time correlated single photon counting technique. The emission decay curves of the N-CDs at 360 nm excitation wavelength are shown in Fig. 6. It can be found that the fluorescence decay remained essentially unchanged after the addition of hypochlorite, suggesting that static quenching occurred mainly in this case [30]. The fluorescence life time for the N-CDs, the N-CDs with  $15\ \mu\text{M}\ \text{ClO}^-$  and the N-CDs with  $27\ \mu\text{M}\ \text{ClO}^-$  was fitted to be 15.24, 15.13, and 14.72 ns, respectively, using single exponential model.

### Detection of free chlorine in real samples

The excellent specificity combined with high sensitivity and selectivity of N-CDs to  $\text{ClO}^-$  suggested that the probe might be directly applied for detecting  $\text{ClO}^-$  in real water samples. Therefore, we further examined the practical application of the assay of  $\text{ClO}^-$  in real samples. The tap water samples obtained from our lab and dormitory (samples 1 and 2) without any pretreatment were spiked with  $\text{ClO}^-$  at different concentration levels, and then analyzed with the established method. The contents of free chlorine in real water samples are summarized in Table 2. The concentration of free residual chlorine in tap water samples 1 and 2 were found to be 0.71 and  $1.40\ \mu\text{M}$ , respectively. The recovery was in the range of 95.7 to 105.0 % with relative standard deviation (RSD) less than 5.39 % ( $n = 3$ ) for all of the samples analyzed. The results indicate that the N-CD-based probe may be a promising assay platform for the detection of  $\text{ClO}^-$  in real environmental samples.

### Conclusions

In summary, we have prepared a kind of nitrogen-doped carbon dots (N-CDs) from citric acid, tartaric acid and ethanediamine by a facile one-pot solvothermal process. The fluorescence of the N-CDs can be effectively quenched by free chlorine and  $\text{ClO}^-$ , and then a method for fluorometric determination of chlorine and hypochlorite was presented.

The strategy is facile, rapid, low cost, and environment friendly, and has a promising prospect in the detection of free chlorine in real samples.

**Acknowledgments** This work was supported by Natural Science Foundation of Fujian Province of China (Nos. 2016Y0065, 2012 J06005 and 2014 J01053), Education Bureau of Fujian Province of China (Nos. JK2011030 and JA13195), and the External Foundation of MOE Key Laboratory of Analysis and Detection for Food Safety (Fuzhou University) (No. FS1307).

**Compliance with ethical standards** The author(s) declare that they have no competing interests.

### References

- Dong Y, Li G, Zhou N, Wang R, Chi Y, Chen G (2012) Graphene quantum dots as a green and facile sensor for free chlorine in drinking water. *Anal Chem* 84:8378–8382
- Wakigawa K, Gohda A, Fukushima S, Mori T, Niidome T, Katayama Y (2013) Rapid and selective determination of free chlorine in aqueous solution using electrophilic addition to styrene by gas chromatography/mass spectrometry. *Talanta* 103:81–85
- Nimkerdphol K, Nakagawa M (2008) Effect of sodium hypochlorite on zebrafish swimming behavior estimated by fractal dimension analysis. *J Biosci Bioeng* 105:486–492
- Aoki T, Munemori M (1983) Continuous flow determination of free chlorine in water. *Anal Chem* 55:209–212
- Japanese Standards Association (2008) Testing Methods for Industrial Wastewater JIS K0102 100–102
- Moberg L, Karlberg B (2000) An improved N,N'-diethyl-p-phenylenediamine (DPD) method for the determination of free chlorine based on multiple wavelength detection. *Anal Chim Acta* 407:127–133
- Marino DF, Ingle Jr., JD (1981) Determination of chlorine in water by luminol chemiluminescence. *Anal Chem* 53: 455–458
- Claver JB, Mirón MCV, Capitán-Vallvey LF (2004) Determination of hypochlorite in water using a chemiluminescent test strip. *Anal Chim Acta* 522:267–273
- Hallaj T, Amjadi M, Manzoori JL, Shokri R (2015) Chemiluminescence reaction of glucose-derived graphene quantum dots with hypochlorite, and its application to the determination of free chlorine. *Microchim Acta* 182:789–796
- Chen P, Wei W-Z, Yao S-Z (1999) Different valency chlorine species analysis by non-suppressed ion-chromatography with double cell quartz crystal detector. *Talanta* 49:571–576
- Watanabe T, Idehara T, Yoshimura Y, Nakazawa H (1998) Simultaneous determination of chlorine dioxide and hypochlorite in water by high-performance liquid chromatography. *J Chromatogr A* 796:397–400
- Pobozy E, Pyrzynska K, Szostek B, Trojanowicz M (1995) Flow-injection spectrophotometric determination of free residual chlorine in waters with 3,3'-dimethylnaphthidine. *Microchem J* 51:379–386
- Ma J, Guo B, Cao X, Lin Y, Yao B, Li F, Weng W, Huang L (2015) One-pot fabrication of hollow cross-linked fluorescent carbon nitride nanoparticles and their application in the detection of mercuric ions. *Talanta* 143:205–211
- Kwon W, Lee G, Do S, Joo T, Rhee S-W (2014) Size-controlled soft-template synthesis of carbon nanodots toward versatile photoactive materials. *Small* 10:506–513

15. Lin L, Rong M, Lu S, Song X, Zhong Y, Yan J, Wang Y, Chen X (2015) A facile synthesis of highly luminescent nitrogen-doped graphene quantum dots for the detection of 2,4,6-trinitrophenol in aqueous solution. *Nanoscale* 7:1872–1878
16. Dong Y, Pang H, Yang H, Guo C, Shao J, Chi Y, Li C, Yu T (2013) Carbon-based dots co-doped with nitrogen and sulfur for high quantum yield and excitation-independent emission. *Angew Chem Int Ed* 52:7800–7804
17. Eda G, Lin Y-Y, Mattevi C, Yamaguchi H, Chen H-A, Chen I-S, Chen C-W, Chhowalla M (2010) Blue photoluminescence from chemically derived graphene oxide. *Adv Mater* 22:505–509
18. Anilkumar P, Wang X, Cao L, Sahu S, Liu J-H, Wang P, Korch K, Tackett KN II, Parenzan A, Sun Y-P (2011) Toward quantitatively fluorescent carbon-based “quantum” dots. *Nanoscale* 3:2023–2027
19. Krysmann MJ, Kellarakis A, Dallas P, Giannelis EP (2012) Formation mechanism of carbogenic nanoparticles with dual photoluminescence emission. *J Am Chem Soc* 134:747–750
20. Zeng X, Yang X, Li F, Ma J, Lin Y, Yao B, Huang L, Weng W (2015) One-step fabrication of nitrogen-doped fluorescent nanoparticles from non-conjugated natural products and their temperature-sensing and bioimaging applications. *Sens Bio-sens Res* 3:18–23
21. Wang D, Xu H, Zheng B, Li Y, Liu M, Du J, Xiao D (2015) N-doped carbon dots with high sensitivity and selectivity for hypochlorous acid detection and its application in water. *Anal Methods* 7:5311–5317
22. Huang Z, Lin F, Hu M, Li C, Xu T, Chen C, Guo X (2014) Carbon dots with tunable emission, controllable size and their application for sensing hypochlorous acid. *J Lumin* 151:100–105
23. Yin B, Deng J, Peng X, Long Q, Zhao J, Lu Q, Chen Q, Li H, Tang H, Zhang Y, Yao S (2013) Green synthesis of carbon dots with down- and up-conversion fluorescent properties for sensitive detection of hypochlorite with a dual-readout assay. *Analyst* 138:6551–6557
24. Ding Y, Ling J, Cai J, Wang S, Li X, Yang M, Zha L, Yan J (2016) A carbon dot-based hybrid fluorescent sensor for detecting free chlorine in water medium. *Anal Methods* 8:1157–1161
25. Xue M, Zhang L, Zou M, Lan C, Zhan Z, Zhao S (2015) Nitro and sulfur co-doped carbon dots: a facile and green fluorescence probe for free chlorine. *Sensors Actuators B Chem* 219:50–56
26. Tang Y, Su Y, Yang N, Zhang L, Lv Y (2014) Carbon nitride quantum dots: a novel chemiluminescence system for selective detection of free chlorine in water. *Anal Chem* 86:4528–4535
27. Shen J, Zhu Y, Yang X, Li C (2012) Graphene quantum dots: emergent nanolights for bioimaging, sensors, catalysis and photovoltaic devices. *Chem Commun* 48:3686–3699
28. Bao L, Zhang Z, Tian Z, Zhang L, Liu C, Lin Y, Qi B, Pang D (2011) Electrochemical tuning of luminescent carbon nanodots: from preparation to luminescence mechanism. *Adv Mater* 23:5801–5806
29. Li L-L, Ji J, Fei R, Wang C-Z, Lu Q, Zhang J-R, Jiang L-P, Zhu J-J (2012) A facile microwave avenue to electrochemiluminescent two-color graphene quantum dots. *Adv Funct Mater* 22:2971–2979
30. Lu Y-C, Chen J, Wang A-J, Bao N, Feng J-J, Wang W, Shao L (2015) Facile synthesis of oxygen and sulfur co-doped graphitic carbon nitride fluorescent quantum dots and their application for mercury(II) detection and bioimaging. *J Mater Chem C* 3:73–78